



signal backscattered from the antenna sensor. As a result, signal backscattered from the sensor can be distinguished from environmental reflections. However, the light-switching mechanism is not practical for outdoor application, where light intensity is usually so strong that the phototransistor is constantly activated and thus, loses ability of switching. To avoid this difficulty, a low-cost off-the-shelf radiofrequency identification (RFID) chip is adopted as a simple mechanism for signal modulation [8]. Since the RFID chip is powered by wireless interrogation signal, the RFID-based strain sensor is wireless and passive (battery-free). The prototype RFID antenna sensor has shown a strain measurement resolution of  $20 \mu\epsilon$  in laboratory experiments, and can measure large strains up to  $10,000 \mu\epsilon$  [9]. Previous studies demonstrated that if operating frequency of the wireless strain sensor is increased, strain sensitivity can be improved and sensor size can be reduced. However, the RFID chip only functions in the frequency band of 860-960MHz. Alternative approaches need to be exploited in order to operate at higher frequencies.

This paper presents a novel wireless strain sensor design that adopts a frequency doubling scheme to enable sensor operation at a high frequency. The basic concept is to let the sensor double the frequency of reader interrogation signal ( $f$ ) and backscatter signal at the doubled frequency ( $2f$ ). Because environmental reflections to reader interrogation signal are concentrated at  $f$ , the reader only receives signal at  $2f$  backscattered from the sensor. The frequency doubling operation is implemented through a Schottky diode, which is a nonlinear circuit device and can generate output signal with frequencies at multiples of input frequency. Diode frequency multipliers have been adopted for energy harvesting [10], insect tracking [11], among others. In [12], a high efficiency diode frequency doubling device is designed using a GaAs Schottky diode that provides 1% conversion efficiency at -30 dBm input power. Nevertheless, the authors are not aware of other literature on using Schottky diode to enable frequency doubling for wireless strain sensing.

In our study, the diode-enabled frequency doubling mechanism is investigated and incorporated with two patch antennas to form a wireless strain sensor. A low-cost Schottky diode (SMS7621-079LF) from Skyworks Solutions, Inc. is adopted. A patch antenna with resonance frequency at 2.9GHz is designed as a receiving antenna of the wireless strain sensor. Meanwhile, another patch antenna with resonance frequency at 5.8GHz is designed to serve as a transmitting antenna of the wireless strain sensor. For connection between these two patch antennas, the simulation model of a Schottky diode is first verified through experimental measurement, and then used to design the matching network between the two patch antennas. Finally, the three components, i.e. the receiving and transmitting antennas and matching network, are combined together to form a frequency doubling antenna sensor. Since operation power of the diode is harvested from wireless interrogation signal, the frequency doubling antenna sensor is wireless and passive (battery-free). Strain sensing simulation shows that the

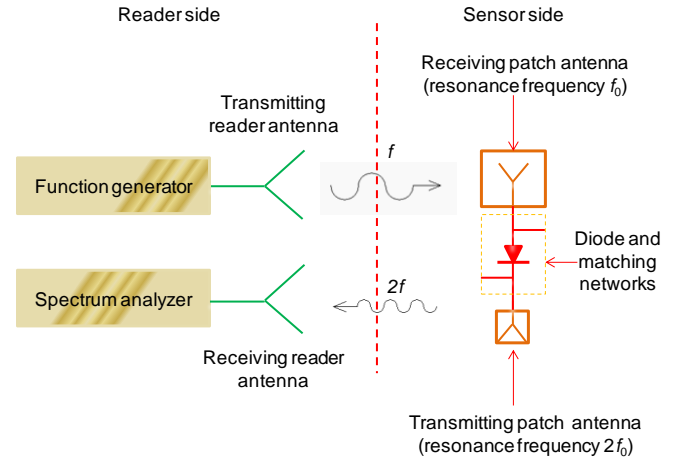


Fig. 1 Operation mechanism of a frequency doubling antenna sensor system

proposed frequency doubling sensor can achieve a strain sensitivity of  $-3.84 \text{ kHz}/\mu\epsilon$ .

The rest of this paper is organized as follows. Strain sensing mechanism of the antenna sensor is first presented. Designs of the 2.9 GHz and 5.8 GHz patch antennas are then described. Next, verification experiment for the Schottky diode simulation model is presented, followed by the diode-integrated matching network design. Combining all three components, simulation results are presented to demonstrate strain sensing performance of the proposed frequency doubling antenna sensor. Finally, a summary and discussion is provided.

## STRAIN SENSING MECHANISM OF FREQUENCY DOUBLING ANTENNA SENSOR

Fig. 1 illustrates the operation mechanism of a frequency doubling antenna sensor. The sensor consists of three main components, i.e., a receiving antenna (with resonance frequency  $f_0$ ), a transmitting antenna (with resonance frequency  $2f_0$ ), and a diode-integrated matching network between receiving and transmitting antennas. During operation, a wireless interrogation signal is emitted from the reader side by a function generator and through a transmitting reader antenna. If interrogation frequency  $f$  is in the neighborhood of  $f_0$ , resonance frequency of the receiving patch antenna at sensor side, interrogation power is captured by the sensor-side receiving patch antenna and transferred to the matching network. The diode then generates output signal at doubled frequency  $2f$ . The output signal at  $2f$  is backscattered to reader through sensor-side transmitting patch antenna (resonance frequency at  $2f_0$ ). A spectrum analyzer finally measures the backscattered signal at reader side. Frequency of backscattered sensor signal is at  $2f$ , and the unwanted environmental reflections to original reader interrogation signal remains at  $f$ . Therefore, it is easy for the

spectrum analyzer to distinguish backscattered sensor signal from unwanted environmental reflections.

The receiving and transmitting antennas of the frequency doubling sensor are microstrip patch antennas. For a microstrip patch antenna with length  $L$ , width  $W$ , and substrate thickness  $h$ , effective dielectric constant of the antenna can be calculated for determining antenna electrical length [13]:

$$\varepsilon_{\text{reff}} = \frac{\varepsilon_r + 1}{2} + \frac{\varepsilon_r - 1}{2} \left[ 1 + 12 \frac{h}{W} \right]^{-\frac{1}{2}} \quad (1)$$

where  $\varepsilon_r$  is the substrate dielectric constant.

The resonance frequency ( $f_0$ ) of a patch antenna at zero strain level can be estimated as:

$$f_0 = \frac{c}{2(L + 2\Delta L)\sqrt{\varepsilon_{\text{reff}}}} \quad (2)$$

where  $c$  is the speed of light;  $\Delta L$  is antenna length compensation due to fringing effect [14], which is given empirically by:

$$\Delta L = 0.412 \frac{(\varepsilon_{\text{reff}} + 0.3) \left( \frac{W}{h} + 0.264 \right)}{(\varepsilon_{\text{reff}} - 0.258) \left( \frac{W}{h} + 0.8 \right)} \quad (3)$$

By defining coefficient  $k$  as:

$$k = 0.412 \frac{(\varepsilon_{\text{reff}} + 0.3) \left( \frac{W}{h} + 0.264 \right)}{(\varepsilon_{\text{reff}} - 0.258) \left( \frac{W}{h} + 0.8 \right)} \quad (4)$$

$\Delta L$  can be rewritten as:

$$\Delta L = kh \quad (5)$$

When the patch antenna is under strain  $\varepsilon$  along the direction of patch length  $L$ , physical dimensions of the patch antenna change accordingly. This change causes shift in resonance frequency:

$$\begin{aligned} f &= \frac{c}{2[L(1 + \varepsilon) + 2kh(1 - \nu\varepsilon)]\sqrt{\varepsilon_{\text{reff}}}} \\ &= \frac{c}{2[(L + 2kh) + (L - 2kh\nu)\varepsilon]\sqrt{\varepsilon_{\text{reff}}}} \\ &\approx f_0 \left( 1 - \frac{L - 2kh\nu}{L + 2kh} \varepsilon \right) = f_0 - S\varepsilon \end{aligned} \quad (6)$$

where  $\nu$  is Poisson's ratio of substrate material;  $S$  represents strain sensitivity of the patch antenna. According to Eq. (6),

when strain is small, resonance frequency change of the patch antenna has an approximately linear relationship with applied strain. This serves as strain sensing mechanism of the patch antenna. In this paper, it is assumed that only receiving antenna of a frequency doubling sensor is bonded to structural surface, while matching network and transmitting antenna are floating and stress/strain free. Through the matching network and transmitting patch antenna, this frequency shift causes change in the backscattered signal, which is to be captured by the reader. This change in the backscattered signal is used to derive strain on the monitored structure.

## FREQUENCY DOUBLING ANTENNA SENSOR DESIGN

This section presents preliminary designs for three components of the frequency doubling antenna sensor, including the receiving antenna, the transmitting antenna, and the diode-integrated matching network. Before diode-integrated matching network is designed, measurement is conducted to verify a simulation model of the diode.

### Receiving and Transmitting Antenna Designs

Substrate material adopted in the preliminary sensor design is Rogers/duroid® 5880, a glass micro-fiber reinforced PTFE material. The substrate thickness is chosen as 31 mil, a trade-off between increasing wireless interrogation distance and improving strain transfer ratio from structural surface to top layer of the microstrip patch antenna [15]. The dielectric constant  $\varepsilon_r$  of the material is 2.2. In current design, the resonance frequency is set to  $f_0 = 2.9\text{GHz}$  for the receiving antenna, and  $2f_0 = 5.8\text{GHz}$  for the transmitting antenna.

The two patch antennas are simulated in a commercial software package, Ansoft HFSS. Fig. 2 shows the photo of a fabricated 2.9GHz patch antenna. The dimension of the antenna is 1.75 in.  $\times$  1.35 in. Fig. 3 shows the simulated scattering parameter  $S_{11}$  plot of the antenna. The simulation shows the antenna has a resonance frequency at 2.9 GHz with return loss  $-40$  dB. The return loss is much lower than the  $-10$  dB return loss threshold for typical antennas, which indicates good radiation performance. Fig. 3 also shows the measured  $S_{11}$  of a

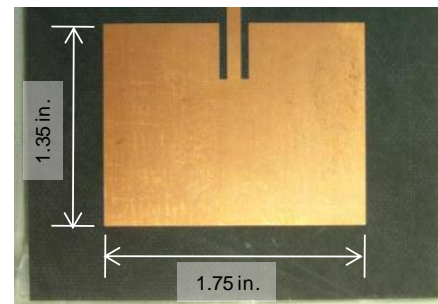


Fig. 2 Photo of a fabricated 2.9GHz receiving patch antenna

piece of fabricated 2.9 GHz receiving antenna. The measured resonance frequency is 2.893GHz, which is about 7MHz (only 0.24% difference) lower than the simulation result. The discrepancy between the simulation and measurement is reasonably small, considering imperfections in both simulation and fabrication. The simulated radiation pattern is plotted in Fig. 4, showing a peak gain of 5.4 dB. The half-power beam-width (HPBW) of the antenna is 76°, which allows flexible reader antenna positioning.

Fig. 5 shows the photo of a fabricated 5.8 GHz transmitting patch antenna. The dimension of the antenna is 0.74 in. × 0.71 in. Fig. 6 shows the  $S_{11}$  plot of the 5.8 GHz transmitting patch antenna. The simulation shows the antenna has a resonance frequency at 5.801 GHz with return loss -23 dB. The

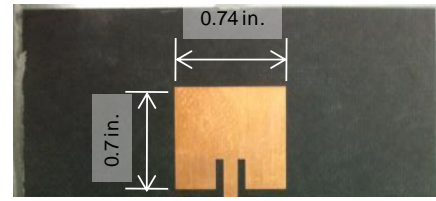


Fig. 5 Photo of a fabricated 5.8GHz transmitting patch antenna

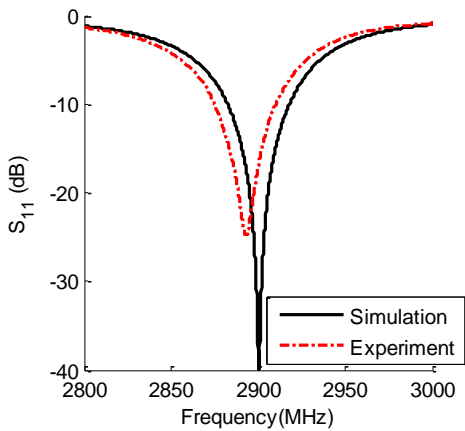


Fig. 3 Simulated and measured  $S_{11}$  of 2.9GHz receiving patch antenna

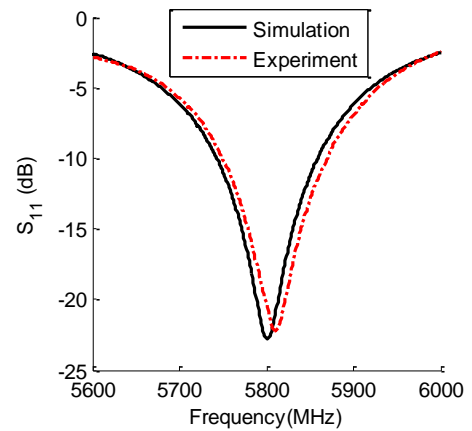


Fig. 6 Simulated and measured  $S_{11}$  of 5.8GHz transmitting patch antenna

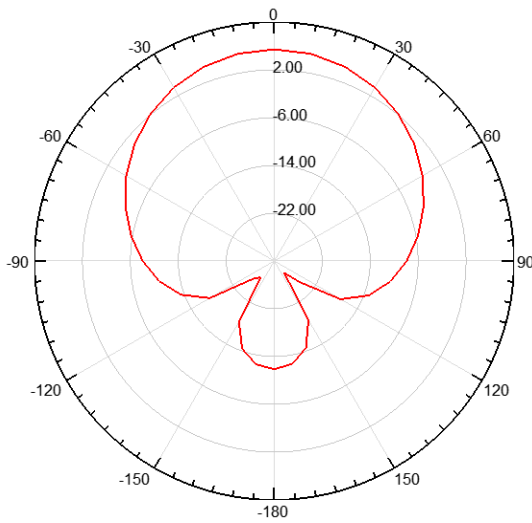


Fig. 4 Simulated radiation pattern of 2.9GHz receiving patch antenna

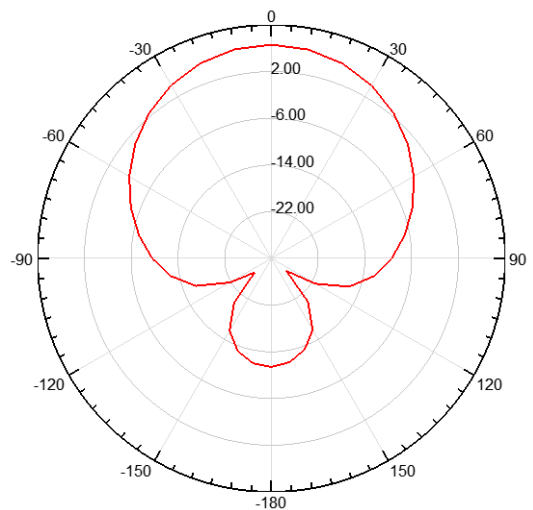


Fig. 7 Simulated radiation pattern of 5.8GHz transmitting patch antenna

measurement of a fabricated piece shows a resonance frequency of 5.81 GHz, i.e. about 9 MHz (only 0.16% difference) higher than the simulation result. The simulated radiation pattern of the antenna is plotted in Fig. 7, showing a peak gain 6.6 dB. The HPBW of the antenna is 67°, which is also convenient for reader antenna positioning.

### Matching Network Design

Besides two patch antennas, diode-integrated matching network between receiving and transmitting antenna is also designed. The goal of matching network design is to maximize output power during frequency doubling. A Schottky diode manufactured by Skyworks Solutions, Inc., the SMS7621-079LF diode, is adopted in this design. A commercial simulation model for this diode, which operates in Advanced Design System (ADS) software package, is provided by Modelithics, Inc. The matching network design is performed in ADS, which has the embedded diode model and built-in microstrip line models. To verify the accuracy of the Modelithics diode model, a diode testing board is first designed and mounted with a Schottky diode (SMS7621-079LF). Performance of the diode is measured and compared with simulation results.

Fig. 8 shows the diode testing board for verifying accuracy of the simulation model. The SMS7621-079LF Schottky diode

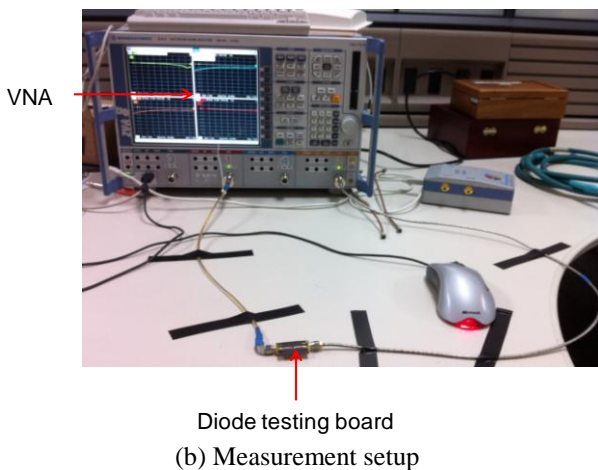
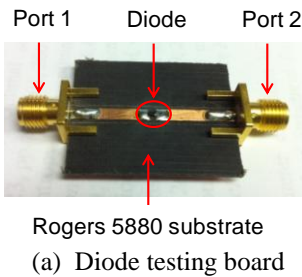
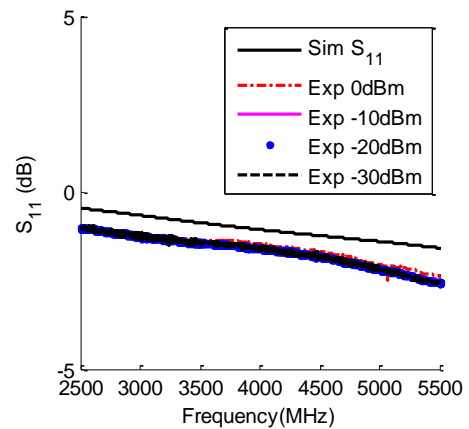
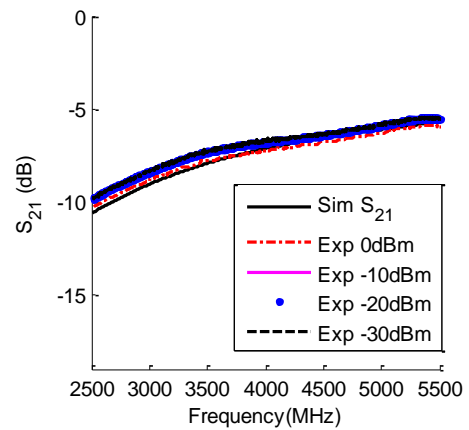


Fig. 8 Experimental setup for diode characterization test

is installed between two 50 Ω transmission lines. Scattering-parameters are measured by vector network analyzer (VNA) when different input power levels are supplied to the board through Port 1. The simulation and experimental results are compared in Fig. 9(a) for S-parameter  $S_{11}$ , and Fig. 9(b) for S parameter  $S_{21}$ . A larger value of  $S_{21}$  means that a higher percentage of the power is transmitted through the matching network. Four different input power levels, 0, -10, -20, and -30 dBm are characterized in the experiments, which are identified in the legend as “Exp 0dBm”, “Exp -10dBm”, “Exp -20dBm”, and “Exp -30dBm”. The simulated S-parameters are also plotted in Fig. 9(a) and Fig. 9(b), which are identified in the legend as “Sim  $S_{11}$ ” and “Sim  $S_{21}$ ”, respectively. For this comparison, a difference within -1dB is regarded as very small, considering fabrication and measurement tolerances, and will have minimum effect to design performance. Close match



(a)  $S_{11}$  comparison



(b)  $S_{21}$  comparison

Fig. 9 Verification for the diode simulation model

between simulation and experimental results indicates the accuracy of simulation model provided by Modelithics, Inc.

The matching network design integrating Schottky diode SMS7621-079LF is then performed in ADS. Fig. 10 shows the photo of a fabricated matching network. The dimension of the matching network is 2.2 in.  $\times$  1.2 in. Because diode is a nonlinear circuit device, power loss of the diode-integrated matching network is dependent on input power level. To verify the input power effect, different input power levels are simulated and the power loss results are summarized in Table 1. In the frequency doubling sensor design, input power of -10 dBm is adopted. At this input power level, power loss due to matching network and diode is the lowest.

To characterize backscattering behavior of the doubling sensor, sensor response for a neighborhood frequency range needs to be analyzed. To this end, power loss due to diode-integrated matching network is investigated by a harmonic balance simulation in ADS. The input power to the matching network is set to -10dBm. The output power at doubled frequency  $2f$  is measured. The results are plotted in Fig. 11.

### STRAIN SENSING PERFORMANCE OF FREQUENCY DOUBLING ANTENNA SENSOR

Three components of the frequency doubling sensor are

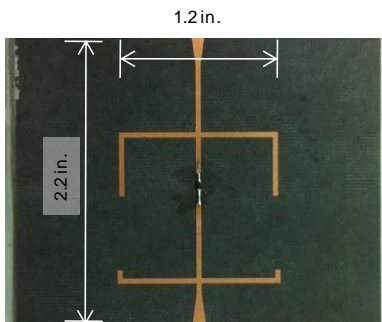


Fig. 10 Photo of matching network in the frequency doubling sensor

Table 1 Simulated power loss under different input power

Input power (dBm)	Output power (dBm)	Power loss due to matching network and diode (dB)
0	-16.932	16.932
-5	-19.855	14.855
-10	-23.602	13.602
-15	-28.712	13.712
-20	-35.533	15.533
-25	-43.287	18.287

combined together and the overall design drawing is shown in Fig. 12. Currently not optimized for size reduction, dimension of the overall frequency doubling antenna sensor is about 4.25 in.  $\times$  1.77 in. Since the physical dimension of a patch antenna is inversely proportional to operating frequency, footprint of the sensor can be easily scaled down by increasing the operating frequency in future designs. The sensor has a power flow mechanism as illustrated in Fig. 13.  $P_0$  represents the received power at the 2.9 GHz receiving antenna.  $P_1$  and  $P_2$  denote the power before and after the matching network, respectively. Finally,  $P$  represents the power being backscattered to the reader. As shown in Fig. 13,  $s_{11}^R$  and  $s_{11}^T$  are scattering-parameters of the receiving and transmitting antennas, respectively. The  $s_{11}^R$  and  $s_{11}^T$  plots of current antenna designs

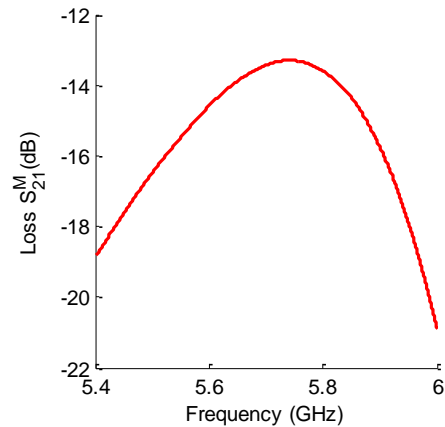


Fig. 11 Power loss of diode-integrated matching network (input power at frequency  $f$ , output power at  $2f$  as marked on the x-axis)

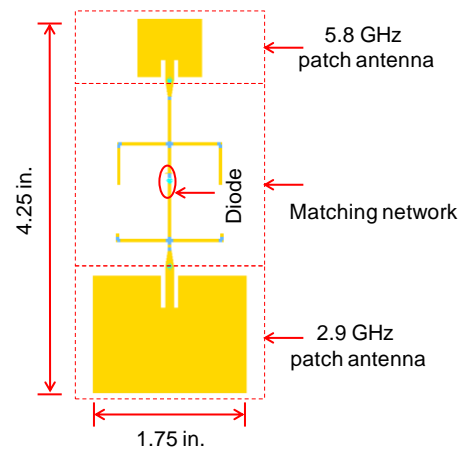


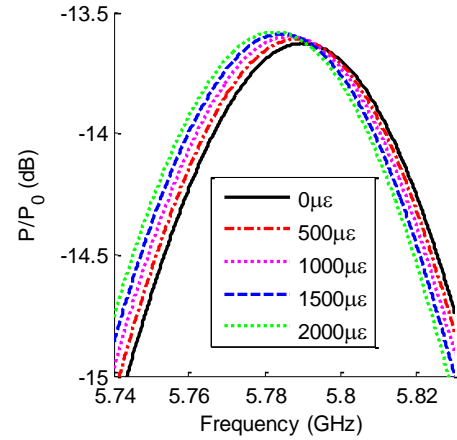
Fig. 12 Design drawing of frequency doubling antenna sensor

have been shown in Fig. 3 and Fig. 6.  $S_{21}^M$  is forward transmission coefficient of the matching network, which determines the ratio of output power at Port 2 over the the input power at Port 1 (as shown in Fig. 11). The overall power  $P$  transmitted back to the reader can be estimated as:

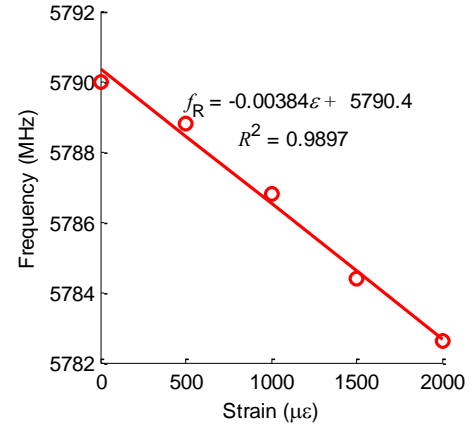
$$P = P_0 (1 - [S_{11}^R]^2) [S_{21}^M]^2 (1 - [S_{11}^T]^2) \quad (7)$$

The  $P/P_0$  ratio, which varies with frequency, quantifies the backscattering performance of the antenna sensor. Combining the individual results for  $S_{11}^R$ ,  $S_{11}^T$ , and  $S_{21}^M$ , the  $P/P_0$  versus frequency relationship is plotted as the solid line ( $0\mu\epsilon$ , i.e. zero strain level) in Fig. 14(a). A clear resonance is demonstrated in the plot, and the corresponding frequency is named as the resonance frequency of the entire sensor. Power loss of the frequency doubling antenna sensor at 5.8 GHz is around  $-13.6$  dBm (for zero strain level). Maximum wireless interrogation distance of the sensor can be estimated according to Friis equation. For this estimation, it is assumed that the interrogation power emitted by the reader-side function generator is 15 dBm, and the lowest backscattered power detectable by the spectrum analyzer is  $-70$ dBm. If both transmitting and receiving antennas at the reader side have a gain of 10 dB, the achievable interrogation distance is estimated to be 2.2m. The distance can be increased during actual testing, e.g. by adopting higher reader interrogation power or reader antennas with higher gain.

When the sensor is under strain, change in the backscattering performance can be interrogated by a wireless reader and used for detecting strain. For simulating the strain sensing performance of the frequency doubling sensor, we studied the scenario when the 2.9 GHz patch antenna is bonded to the monitored structure and stretched under strain. All other parts of the sensor, including the matching network and the 5.8 GHz transmitting antenna, are strain free. Four more strain levels, from  $500\mu\epsilon$  to  $2,000\mu\epsilon$  with  $500\mu\epsilon$  increment, are simulated. The relationship between power ratio  $P/P_0$  and frequency at each strain level is again plotted in Fig. 14(a). Resonance frequency of the entire sensor is shown to decrease as strain increases. The resonance frequency at each strain level



(a) Power ratio  $P/P_0$  versus frequency relationship for multiple strain levels



(b) Resonance frequency (of the entire sensor) versus strain relationship

Fig. 14 Strain sensing simulation results for the frequency doubling antenna sensor

is extracted from Fig. 14(a), and plotted against strain in Fig. 14(b). The figure shows a simulated strain sensitivity at  $-3.84$  kHz/ $\mu\epsilon$ , which is about five times higher than the RFID-based antenna sensor presented in [8].

## CONCLUSIONS

In this research, a passive frequency doubling antenna sensor is designed and fabricated. A Schottky diode is integrated in the sensor design for generating output signal at doubled frequency of the input signal, which allows the reader to easily distinguish backscattered sensor signal from unwanted environmental reflections. Because operation power of the diode is captured from wireless interrogation signal emitted by a reader, no other power source is needed by the sensor, which means the antenna sensor is wireless and passive (battery-free).

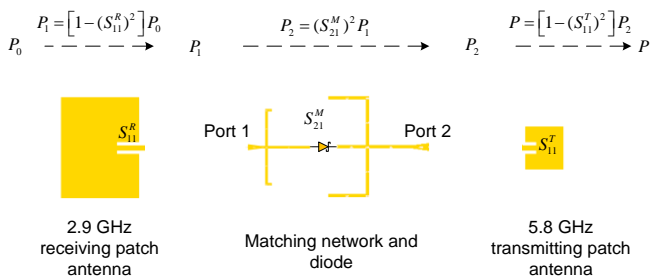


Fig. 13 Power flow of frequency doubling antenna sensor

Two patch antennas, serving as 2.9GHz receiving antenna and 5.8GHz transmitting antenna, are designed. A Schottky diode simulation model is first verified by measurement, and then used for designing the diode-integrated matching network. The three components of the frequency doubling antenna sensor are combined together and the strain sensing performance is simulated. Based on simulation results, a strain sensitivity of  $-3.84 \text{ kHz}/\mu\epsilon$  is achieved. Tensile testing will be performed in the future to evaluate the strain sensing performance of the frequency doubling sensor.

## ACKNOWLEDGMENTS

This material is based upon work supported by the Federal Highway Administration under agreement No. DTFH61-10-H-00004. Any opinions, findings, and conclusions or recommendations expressed in this publication are those of the authors and do not necessarily reflect the view of the Federal Highway Administration. The authors would like to acknowledge the Modelithics models utilized under the University License Program from Modelithics, Inc., Tampa, FL.

## REFERENCES

- [1] H. Sohn, C. R. Farrar, F. M. Hemez, D. D. Shunk, D. W. Stinemat, and B. R. Nadler, "A Review of Structural Health Monitoring Literature: 1996-2001," Report No. LA-13976-MS, Los Alamos National Laboratory, Los Alamos, NM, 2003.
- [2] M. Çelebi, "Seismic Instrumentation of Buildings (with Emphasis on Federal Buildings)," Report No. 0-7460-68170, United States Geological Survey, Menlo Park, CA, 2002.
- [3] S. John C., G. Jun, C. Nattapon, K. Wen H., and Y. Darrin J., "Wireless, passive, resonant-circuit, inductively coupled inductive strain sensor," *Sensors and Actuators A*, vol. 102, pp. 61-66, 2002.
- [4] K. J. Loh, J. P. Lynch, and N. A. Kotov, "Inductively coupled nanocomposite wireless strain and pH sensors," *Smart Structures and Systems*, vol. 4, pp. 531-548, 2008.
- [5] Y. Jia, K. Sun, F. J. Agosto, and M. T. Quinones, "Design and characterization of a passive wireless strain sensor," *Measurement Science and Technology*, vol. 17, pp. 2869-2876, 2006.
- [6] K. Finkenzerler, *RFID Handbook*, 2nd ed., John Wiley & Sons, New York, 2003.
- [7] S. Deshmukh and H. Huang, "Wireless interrogation of passive antenna sensors," *Measurement Science and Technology*, vol. 21, pp. 035201, 2010.
- [8] X. Yi, T. Wu, Y. Wang, R. T. Leon, M. M. Tentzeris, and G. Lantz, "Passive wireless smart-skin sensor using RFID-based folded patch antennas," *International Journal of Smart and Nano Materials*, vol. 2, pp. 22-38, 2011.
- [9] X. Yi, T. Wu, G. Lantz, J. Cooper, C. Cho, Y. Wang, M. M. Tentzeris, and R. T. Leon, "Sensing resolution and measurement range of a passive wireless strain sensor," Proceedings of the 8th International Workshop on Structural Health Monitoring, Stanford, CA, USA, 2011.
- [10] S. Berndie and C. Kai, "5.8-GHz circularly polarized rectifying antenna for wireless microwave power transmission," *IEEE Transactions on Microwave Theory and Techniques*, vol. 50, pp. 1870-1876, 2002.
- [11] C. Bruce G. and B. Gilles, "Harmonic radar transceiver design: miniature tags for insect tracking," *IEEE Transactions on Antennas and Propagation*, vol. 52, pp. 2825-2832, 2004.
- [12] P. Suzette M., W. Thomas M., S. Steven, and R. Michael, "High efficiency diode doubler with conjugate-matched antennas," Proceedings of the 37th European Microwave Conference, Munich, 2007.
- [13] C. A. Balanis, *Antenna Theory: Analysis and Design*, 2nd ed., John Wiley & Sons, New York, 1997.
- [14] I. J. James and P. S. Hall, *Handbook of Microstrip Antennas*, Peter Peregrinus Ltd., 1989.
- [15] X. Yi, T. Wu, G. Lantz, Y. Wang, R. T. Leon, and M. M. Tentzeris, "Thickness variation study of RFID-based folded patch antennas for strain sensing," Proceedings of SPIE, Sensors and Smart Structures Technologies for Civil, Mechanical and Aerospace Systems, San Diego, CA, USA, 2011.